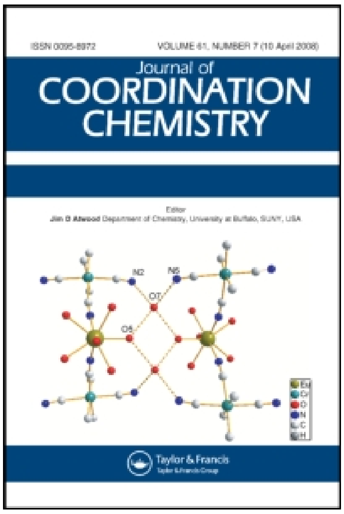

Journal of Coordination Chemistry
Publication details, including instructions for authors and subscription information:
http://www.informaworld.com/smpp/title~content=t713455674

MOLECULAR ORBITAL ANALYSIS OF NUCLEOPHILIC ATTACK ON A PLATINUM ALLYL COMPLEX

J. S. Haley[a]; M. C. Milletti[a]
[a] Department of Chemistry, Eastern Michigan University, Ypsilanti, MI

To cite this Article Haley, J. S. and Milletti, M. C.(2001) 'MOLECULAR ORBITAL ANALYSIS OF NUCLEOPHILIC ATTACK ON A PLATINUM ALLYL COMPLEX', Journal of Coordination Chemistry, 52: 4, 345 — 360

To link to this Article: DOI: 10.1080/00958970108028183

URL: http://dx.doi.org/10.1080/00958970108028183

J. Coord. Chem., 2001, Vol. 52, pp. 345-360
Reprints available directly from the publisher
Photocopying permitted by license only

Published by license under
the Gordon and Breach Science
Publishers imprint.
Printed in Malaysia.

MOLECULAR ORBITAL ANALYSIS OF NUCLEOPHILIC ATTACK ON A PLATINUM ALLYL COMPLEX

J. S. HALEY and M. C. MILLETTI*

Department of Chemistry, Eastern Michigan University, Ypsilanti, MI 48197

(Received 21 January 2000; In final form 21 April 2000)

The platinum allyl complex, $[(\eta^3\text{—}CH_2C(CH_3)C{=}CH_2)Pt(PPh_3)_2]^+$, behaves differently toward nucleophiles depending on their hardness. In the reaction with a "hard" nucleophile, nucleophilic attack occurs at the metal center. A "soft" nucleophile bonds to the middle carbon of the allyl ligand. The results of molecular orbital calculations suggest that both reactions are orbital controlled, which points to the metal as the preferred site of attack. However, the soft nucleophile attacks the allyl ligand due to steric constraints. A Mulliken population analysis reveals that the platinum center is directly bonded to only the two end carbons of the allyl ligand. The effect of basis set size and substitution of hydrogens for phenyl groups on the results of the calculations was also investigated. The choice of basis set had the largest effect on the charge distribution of the molecule. On the other hand, basis set size and inclusion of phenyl substituents on the phosphine ligands had minimal effect on the optimized structure of the complex.

Keywords: Molecular orbital calculations; Nucleophilic attack; Allyl; Hard nucleophile; Soft nucleophile

INTRODUCTION

The platinum allyl complex, $[(\eta^3\text{—}CH_2C(CH_3)C{=}CH_2)Pt(PPh_3)_2]^+$, is of interest due to its unusual behavior toward hard and soft nucleophiles [1]. When the complex is allowed to react with a "hard" nucleophile such as the cyanoborate ion, in the resulting product the nucleophile bonds directly to platinum, suggesting that nucleophilic attack is occurring at the metal

---

*Corresponding author. Tel.: 313 487 0106, Fax: 313 487 1496, e-mail: milletti@online.emich.edu

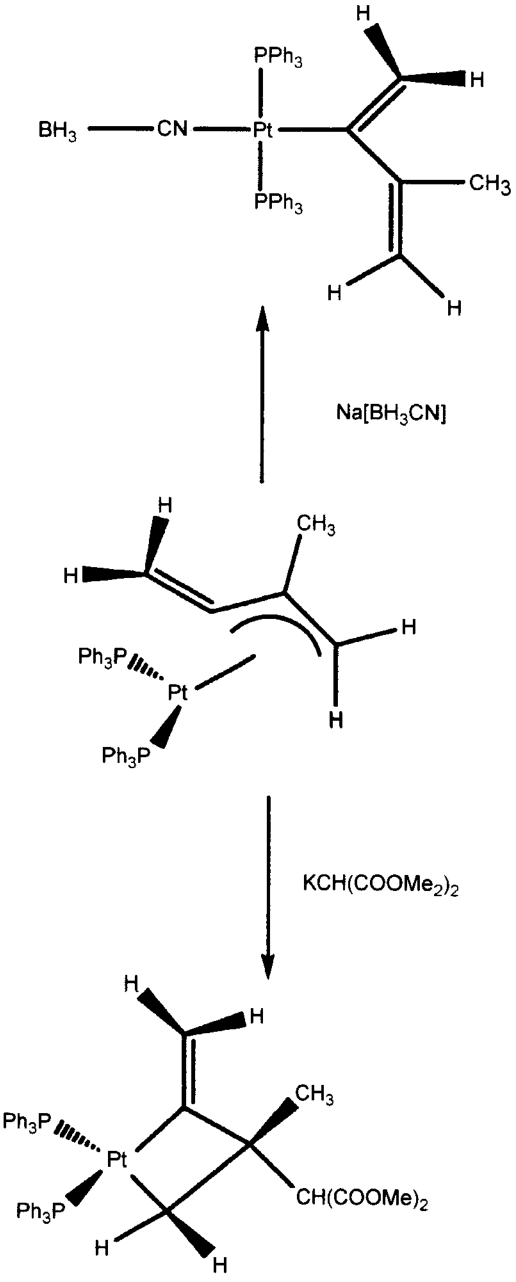
BH3
CN
Pt
PPh3
PPh3
CH3
H
H
H
H
Na[BH3CN]
H
H
CH3
H
H
Ph3P
Pt
Ph3P
KCH(COOMe2)2
H
H
CH3
Ph3P
Pt
Ph3P
CH(COOMe)2
H
H

SCHEME 1

center. A "soft" nucleophile, such as the malonate ion, reacts with the complex to form a product in which the nucleophile is bonded to the middle carbon of the allyl ligand (see Scheme 1).

The structure of the complex has been experimentally determined [1] and it shows that three of the carbon atoms in the butadienyl ligand are bonded to the metal in an η^3-allyl fashion. The allyl moiety is in conjugation with another C to C double bond, leading to π delocalization. When a complex with this type of structure is attacked by a nucleophile, attack usually occurs at one of the terminal carbons away from the face of the allyl and away from the metal [2].

The purpose of this work is to determine the site of nucleophilic attack on the platinum complex and how it depends on the type of nucleophile (hard or soft). Reactions of this type can be classified as orbital or charge controlled [3]. To determine if a reaction is orbital controlled, the energy difference between the HOMO of the nucleophile and LUMO of the substrate must be considered. If the difference is small the reaction can be said to be orbital controlled; if the difference is large it is charge controlled. In the charge controlled case, the nucleophile attacks at the site of largest positive charge on the substrate; in the orbital controlled case the nucleophile attacks at the LUMO of the substrate [4]. Determination of whether the hard and soft nucleophiles listed above react with the platinum complex in a charge or orbital controlled fashion will lead to the identification of the site of attack on the substrate for each of the nucleophiles.

To address the question detailed above, molecular orbital calculations were carried out on the substrate, $[(\eta^3\text{—}CH_2C(CH_3)C{=}CH_2)Pt(PPh_3)_2]^+$, and the two nucleophiles, the dimethyl malonate ion and the cyanoborate ion. In addition to determination of the site of attack, the effects of method of calculation, basis set size, and substituting hydrogens for bulkier groups on the results of the calculations were also investigated.

DETAILS OF THE CALCULATIONS

The GAUSSIAN94 suite of programs was used to carry out all molecular orbital calculations [5]. Calculations were performed on a DEC Alpha 2100 cluster, except for the largest substrate calculation (HF2MBopt2MBϕ), for which the Pittsburgh Supercomputing Center Digital Alpha 3000 and DEC station 5000 systems were employed. Below is a description of all calculations performed. Details of the six calculations performed on the substrate complex are summarized in Table I.

TABLE I Summary of the six calculations on the substrate complex

Calculation	*Method*	*Basis set*	*Geometry opt.*	*PPh_3 or PH_3*
HF2MBopt2MB	HF	LANL2MB	Yes	PH_3
HF2DZopt2MB	HF	LANL2DZ	No	PH_3
Xα2MBopt2MB	Xα	LANL2MB	No	PH_3
Xα2DZopt2MB	Xα	LANL2DZ	No	PH_3
HF2DZopt2DZ	HF	LANL2DZ	Yes	PH_3
HF2MBopt2MBϕ	HF	LANL2MB	Yes	PPh_3

Calculation HF2MBopt2MB

This first *ab initio* Hartree–Fock calculation included a complete geometry optimization [6] using the available X-ray data [7] for the complex as a starting point; a LANL2MB [8] basis set was used for the metal and an STO-3G [9, 10] basis set was used for the other atoms in the molecule.

Calculations HF2DZopt2MB, Xα2MBopt2MB, Xα2DZopt2MB

The optimized geometry obtained from calculation HF2MBopt2MB was then used for three additional calculations: HF2DZopt2MB using the HF method [11] and a LANL2DZ [8] basis set; Xα2MBopt2MB using the Xα method [12, 13] and a LANL2MB basis set; Xα2DZopt2MB using the Xα method and a LANL2DZ basis set. These four calculations were performed in order to investigate the effects of choice of method and basis set size on the results.

Xα is a DFT method, in which the exact HF exchange for a single determinant is replaced by a more general exchange-correlation functional. This functional includes terms accounting for both exchange energy and electron correlation. In the Xα exchange functional $\rho^{4/3}$ is used with the empirical coefficient of 0.7 [14].

The LANL2MB and LANL2DZ basis sets both employ an effective core potential. The LANL2MB basis uses a minimal basis (MB) set (STO-3G), while LANL2DZ uses a D95 basis on the first row elements and a full double zeta (DZ) set of functions on the other elements. By employing the use of an effective core potential, it is possible to do molecular orbital calculations on molecules containing atoms of significant size, such as platinum. The effective core potential has been derived relativistically [8].

Calculation HF2DZopt2DZ

A fifth calculation was carried out by performing a complete geometry optimization from the same initial set of structural data as in calculation

HF2MBopt2MB, followed by an *ab initio* HF calculation utilizing a LANL2DZ basis set. This calculation was performed in order to determine whether the optimized geometry of the structure would be different at a higher basis set level.

Calculation HF2MBopt2MBϕ

Calculations HF2MBopt2MB and HF2DZopt2DZ were performed with the six phenyl rings on the two phosphine ligands replaced by six hydrogens. Hydrogens are often used to replace large groups with similar electronic behavior to decrease the computational time needed for calculation [15]. Calculation HF2MBopt2MBϕ was performed to investigate the validity of such substitutions and included all phenyl groups. Because of the number of basis functions involved, the calculation was done on the Supercluster of Alpha processors at the Pittsburgh Supercomputing Center. In this calculation, X-ray crystal data obtained from the literature [7] was the starting point of a geometry optimization followed by an HF/LANL2MB calculation.

Nucleophiles

Calculations were also done on the two nucleophiles, dimethyl malonate ion and cyanoborate ion. For each nucleophile a geometry optimization followed by an HF calculation was performed at the LANL2DZ basis set level.

RESULTS AND DISCUSSION

Calculation HF2MBopt2MB

The optimized structure of the platinum complex from calculation HF2MBopt2MB shows that the complex is essentially square planar, making it possible for a nucleophile to attack above and below the plane of the molecule. Table II includes selected bond lengths and angles and Figure 1 shows the position and numbering scheme for a few selected atoms. The C10–C13–C14 angle is 110.44°, not quite a full 120.0° as expected for an sp^2 carbon; the bond lengths for carbons 10 to 13 and from 13 to 14 are only different by one hundredth of an angstrom. The C14–C15 length is in good agreement with carbon to carbon double bonds, while carbons 13 and 18 are well within experimental single bond lengths. Among the platinum to

TABLE II Comparison of selected bond lengths and angles between crystal structure data and calculations HF2MBopt2MB, HF2DZopt2DZ and HF2MBopt2MBϕ

Calculation	2*MB*	2*DZ*	ϕ	*X-ray data* [7]
Bond lengths (Å)				
Pt-P2	2.666	2.492	2.635	2.299
Pt-P6	2.621	2.435	2.593	2.294
Pt-C10	2.177	2.258	2.228	2.20
Pt-C13	2.316	2.320	2.319	2.20
Pt-C14	2.066	2.081	2.072	2.09
Pt-C15	3.164	3.203	3.202	3.19
C10-C13	1.425	1.409	1.408	1.42
C13-C14	1.435	1.437	1.442	1.44
C14-C15	1.308	1.322	1.308	1.26
C13-C18	1.526	1.509	1.526	1.56
Bond Angles				
P2-Pt-P6	91.42	99.56	99.18	100.3
P2-Pt-C10	99.63	96.79	96.26	94.2
P6-Pt-C14	101.66	97.42	98.04	NA
C10-Pt-C14	67.16	66.17	66.57	69.1
C10-C13-C14	110.44	112.91	112.00	117.0
C13-C14-C15	140.96	140.18	137.73	141.0
Pt-C13-C18	126.54	123.74	125.83	NA
Torsion Angles				
C10-C13-C14-C15	128.41	125.60	−127.54	137.06
C15-C14-C13-C18	−68.12	−70.66	67.88	53.75

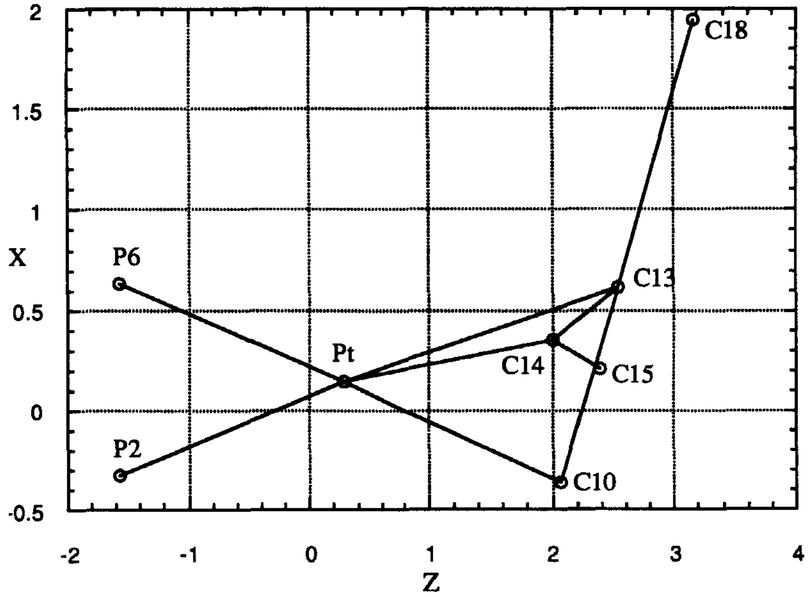

FIGURE 1 View of the complex in the $x-z$ plane showing the numbering scheme.

carbon bond distances, that to carbon 13 is the longest (2.32 Å), that to carbon 14 is the shortest (2.06 Å), and that to carbon 10 is 2.18 Å.

An analysis of the molecular orbitals in the complex shows that the HOMO is a delocalized π bond among the platinum center, C14 and C15. In the LUMO, the platinum is π^* to C15 and C13 has its orbital directed toward the platinum in a σ fashion. An overall view of the molecule's bonding scheme shows that there are four σ and three π carbon-to-carbon bonding orbitals. The platinum to butadienyl ligand bonding is comprised of two σ and three π orbitals.

Table III lists Mulliken overlap populations [16] between relevant atom pairs and compares them to the respective bond lengths. In general, large positive overlap populations indicate a stronger bond and correlate with shorter bond distances. The data suggest that there is no bonding interaction between the platinum center and C13, C15 and C18; however, there is significant overlap between the metal and C14 and C10. Furthermore, there is considerably more overlap between C14–C15 than C13–C18. This is not unexpected since these are formally double and single bonds, respectively. The C10–C13 and C13–C14 overlap populations suggest a delocalized double bond holding together the three allylic carbons. From these data it can be concluded that the platinum center is directly bonded to only two of the butadienyl carbons.

Calculations HF2DZopt2MB, Xα2MBopt2MB, Xα2DZopt2MB

The purpose of the four calculations was to compare two different molecular orbital methods (HF *vs.* Xα) and two different basis sets (LANL2MB *vs.* LANL2DZ).

TABLE III Mulliken population analysis for all calculations on the platinum substrate

	Bond	*LANL2MB*		*LANL2DZ*		*LANL2DZ*	*LANL2MB*
Bond	*length*	*HF*	*Xα*	*HF*	*Xα*	*opt 2DZ*	ϕ
Pt–P2	2.67	0.047	0.072	0.184	0.174	0.212	0.092
Pt–P6	2.62	0.052	0.081	0.179	0.177	0.208	0.101
Pt–C10	2.18	0.127	0.130	0.172	0.158	0.152	0.109
Pt–C13	2.32	−0.076	−0.130	−0.105	−0.053	−0.0889	−0.0762
Pt–C14	2.07	0.202	0.208	0.110	0.151	0.100	0.208
Pt–C15	3.16	0.026	−0.027	−0.022	0.005	−0.0152	−0.028
C10–C13	1.42	0.468	0.459	0.329	0.362	0.389	0.491
C13–C14	1.43	0.454	0.454	0.324	0.402	0.312	0.448
C13–C18	1.53	0.364	0.379	0.270	0.309	0.275	0.614
C14–C15	1.31	0.612	0.607	0.478	0.440	0.476	0.366

Table III shows a comparative Mulliken population analysis for calculation HF2MBopt2MB and the single point calculations HF2DZopt2MB, Xα2MBopt2MB, Xα2DZopt2MB. All calculations show either a very small or a negative value for the overlap population between Pt and C13, suggesting an antibonding, or at best a non-bonding interaction. Also in all calculations the metal has the largest overlap with C10 and C14. In the butadienyl ligand, all calculations yield a large overlap population between C14 and C15, suggesting a double bond between these two centers. The smallest carbon–carbon overlap population in all calculations is between C13 and C18, suggesting a normal single bond. The overlap between C10 and C13 and between C13 and C14 has values which are intermediate between that of a single and that of a double bond. This indicates a delocalization of the π electron density among the three atoms, typical of an allyl-type ligand.

In general, the two calculations at the higher basis set level (LANL2DZ) show the Pt-C10 and Pt-C14 bonds to be more or less equivalent; while both LANL2MB calculations suggest that the Pt-C14 bond is stronger than the Pt-C10 bond. In terms of bonding within the butadienyl ligand, the LANL2MB calculations indicate that there is a clear distinction between the C13–C18 bond (on average an overlap of $0.37\,e^-$), the C10–C13 and C13–C14 bonds (on average $0.46\,e^-$), and the C14–C15 bond ($0.61\,e^-$). This distinction is less pronounced for the calculations employing the larger basis set, where the C13–C18 overlap is $0.29\,e^-$, the C10–C13 and C13–C14 overlaps are $0.35\,e^-$ and the C14–C15 overlap is $0.46\,e^-$. Therefore, the LANL2DZ calculations seem to imply more delocalized bonding within the butadienyl ligand than the LANL2MB calculations. Another difference between the two basis sets is in the bonding between the metal and the phosphine ligands: the lower basis set calculations show very little bonding between Pt and either P atom, while the higher basis set calculations indicate a clear single bond. Figure 2 summarizes this analysis by showing the bonding suggested by the results of each calculation.

Table IV shows partial atomic charges on each center from each of the four calculations. There are significant differences among the four calculations. For example, the Xα calculations Xα2MBopt2MB and Xα2DZopt2MB place the most positive charge on the H atoms of the butadienyl ligand. Calculation HF2MBopt2MB shows the metal to have the most positive charge (0.228), while C13 has a charge of 0.103. When a higher basis set is used, as in calculation HF2DZopt2MB, then C13 of the butadienyl ligand has the most positive charge (0.323) and the metal has a charge of 0.105. Also, with the larger basis set, the charge

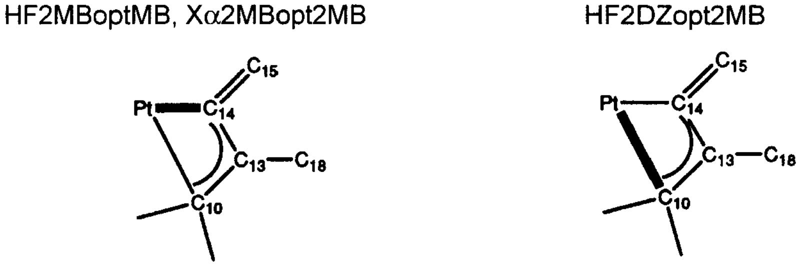

Xα2DZoptMB

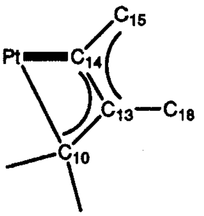

FIGURE 2 Interaction between the metal and the butadienyl ligand as suggested by calculations HF2MBopt2MB, HF2DZopt2MB, Xα2MBopt2MB, Xα2DZopt2MB.

TABLE IV Charge distribution for all calculations on the platinum substrate. Bold numbers indicate the sites of most positive charge for non-hydrogen atoms

Atom	*LANL2MB*		*LANL2DZ*		*LANL2DZ*	*LANL2MB*
calc.	*HF*	*Xα*	*HF*	*Xα*	*opt 2DZ*	*ϕ*
1. Pt	**0.288**	**0.045**	0.105	−0.042	−0.061	0.051
2. P	−0.333	−0.362	0.181	−0.023	0.268	−0.035
3. H	0.158	0.182	0.040	0.120	0.046	−0.028
4. H	0.157	0.183	0.038	0.119	0.028	−0.023
5. H	0.159	0.192	0.048	0.129	0.046	−0.024
6. P	−0.326	−0.354	0.198	−0.004	0.302	−0.025
7. H	0.159	0.191	0.042	0.124	0.053	−0.027
8. H	0.160	0.192	0.043	0.124	0.032	−0.021
9. H	0.159	0.192	0.050	0.128	0.045	−0.029
10. C	−0.137	−0.180	−0.547	−0.646	−0.542	−0.139
11. H	0.112	0.153	0.247	0.309	0.248	0.122
12. H	0.132	0.175	0.270	0.330	0.277	0.105
13. C	0.103	**0.063**	**0.323**	**0.247**	**0.336**	**0.083**
14. C	−0.010	0.011	−0.094	0.087	−0.107	−0.017
15. C	−0.082	−0.157	−0.455	−0.657	−0.456	−0.099
16. H	0.109	0.148	0.213	0.268	0.205	0.095
17. H	0.112	0.153	0.221	0.294	0.226	0.101
18. C	−0.186	−0.283	−0.593	−0.770	−0.606	−0.181
19. H	0.108	0.147	0.222	0.288	0.219	0.101
20. H	0.110	0.150	0.231	0.295	0.232	0.099
21. H	0.103	0.141	0.209	0.277	0.208	0.095

on the butadienyl carbons becomes more positive, regardless of the method.

Depending on the method used, the charge on the metal changes from positive (HF) to essentially neutral ($X\alpha$), confirming what has been noted in the literature [17]. It has been observed that the partial charge on the metal in a transition metal complex often depends on the method used; using $X\alpha$ leads to a negative or smaller positive charge for the metal then if a HF method (*ab initio*) is employed. The $X\alpha$ method has been found to be consistent with experiment when predicting the charge on atoms in a molecule [17a], unlike results obtained with the HF method [18].

Two possible reasons are usually given for the difference between the two methods: the first is that the LCAO (linear combination of atomic orbitals) basis set used for the heavier atoms is generally worse than the basis set used in the lighter atoms; the second is the approximation made in the Mulliken population analysis that the electrons shared in the bond are equally apportioned between the two centers [17a]. The effect of the basis set has been minimized in calculations $X\alpha$2DZopt2MB and HF2DZopt2MB, while the Mulliken approximation remains in calculations HF2MBopt2MB and HF2DZopt2MB.

Even though in Table IV the hydrogen atoms are shown to carry most of the positive charge in the $X\alpha$ calculations, they cannot be considered as possible sites of nucleophilic attack. When non-hydrogen atoms are considered, all calculations but HF2MBopt2MB show C13 as the center carrying the most positive charge. The charge distribution in calculation HF2MBopt2MB points to the metal as the site of most positive charge, due to the problems of HF calculations with a smaller basis set discussed above.

Another comparison that can be made among the four calculations is to consider the values for the energy and position of the LUMO. Table V shows the composition of the LUMO for all calculations and the sum of the contributions for each type of ligand and the metal. In all calculations the metal has the largest single contribution, with the butadienyl ligand also carrying a significant share of the LUMO. The general conclusion is that the LUMO is delocalized between the metal and the butadienyl ligand.

Calculation HF2DZopt2DZ

The purpose of this calculation was to investigate whether employing a higher basis set has an effect on the optimized structure of the complex. For this calculation, the starting coordinates are the same as in calculation

TABLE V Total contributions to the LUMO of the complex for calculations on the platinum substrate

	LANL2MB		*LANL2DZ*		*LANL2DZ*	*LANL2MB*
Atom	*HF*	*Xα*	*HF*	*Xα*	*opt2DZ*	*ϕ*
Pt	1.628	1.778	2.266	1.812	1.971	2.193
P(2)	0.110	0.306	0.685	0.712	0.497	0.140
P(6)	0.118	0.546	0.492	0.768	0.521	0.121
Phosphines	0.228	0.852	1.177	1.48	1.018	0.261
C(10)	0.318	0.378	0.693	0.613	0.632	0.395
C(13)	0.296	1.083	1.096	1.470	0.937	0.433
C(14)	0.127	0.352	0.716	0.796	0.556	0.117
C(15)	0.463	0.670	1.028	0.962	0.823	0.614
C(18)	0.197	0.121	0.307	0.279	0.384	0.215
Butadienyl	1.401	2.604	3.84	4.12	3.332	1.774

HF2MBopt2MB, but the optimization was carried out at the LANL2DZ level.

Shown in Table II is a comparison between the X-ray crystal structure bond lengths and angles [7] and those from calculations HF2MBopt2MB and HF2DZopt2DZ. The two calculations, unlike the crystal structure data, indicate that the two phosphine ligands are not equivalent. However, the distances between the platinum center and the allyl carbons are essentially the same in both the crystal structure and the calculations and, overall, the higher basis set did not have a significant effect on the complex's optimized bond lengths.

The size of the basis set is seen to have a larger effect on the optimized bond angles. Significant differences appear in the values for the P–Pt–P angle, the P2–Pt–C10 angle, and the bond angle for the allyl portion of the butadienyl ligand. In general, optimized values for the higher basis set calculation are closer to the experimental bond angles.

Table III shows a comparison of overlap populations between calculations HF2MBopt2MB and HF2DZopt2DZ. Optimization at the higher basis set level does not change significantly the pattern of overlap populations. The bonding between the metal and the butadienyl ligand as determined in calculation HF2DZopt2DZ also indicates delocalized electron density among carbons 10, 13, and 14 (see Fig. 3).

The charge distribution for calculation HF2DZopt2DZ is shown in Table IV. The metal shows a slight negative charge while the butadienyl ligand carbon 13 is the site carrying the most positive charge. This result does not agree with the results obtained in calculation HF2MBopt2MB, but it is consistent with the other LANL2DZ calculations (see Tab. IV).

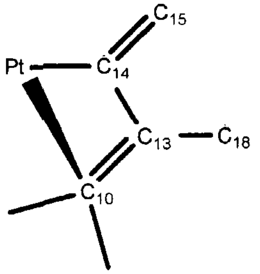

FIGURE 3 Interaction between the metal and the butadienyl ligand as suggested by calculation HF2DZopt2DZ.

Shown in Table V are the contributions to the LUMO from HF2DZopt2DZ; the data indicate that the metal has the largest contribution, while carbons 13 and 15 have the second and third highest.

In conclusion, optimization using a higher basis set has a minor effect on the optimized structure of the complex. The metal-to-ligand bonding in calculation HF2DZopt2DZ is similar to that of calculation HF2DZopt2MB.

Calculation HF2MBopt2MBϕ

Calculation HF2MBopt2MBϕ was done to determine the effect of substituting hydrogens for phenyl rings on the structure and bonding of the complex.

Table II shows a comparison of bond lengths and angles among the X-ray structure, calculation HF2MBopt2MB and calculation HF2MBopt2MBϕ. There are no significant differences in bond lengths between the two calculations, while bond angles seem more sensitive to changes in the input. Bond angles in calculation HF2MBopt2MBϕ are closer to the X-ray structure angles, except for the C13–C14–C15 angle, which is 141.0° in both calculation HF2MBopt2MB and the X-ray structure, but 138.0° in calculation HF2MBopt2MBϕ. In summary, inclusion of the phosphine phenyl rings has very little effect on the geometry of the molecule.

A comparison between the overlap populations of calculation HF2MBopt2MB and those of calculation HF2MBopt2MBϕ can be made from the values in Table III. Except for a slight increase in the overlap population between Pt and the two phosphorus atoms (due to a shortened bond distance between these atoms), other overlap populations remained essentially the same. Figure 4 shows the bonding between the metal and the organic ligand suggested by calculation HF2MBopt2MBϕ.

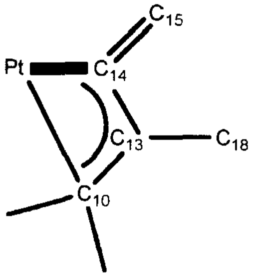

FIGURE 4 Interaction between the metal and the butadienyl ligand as suggested by calculation HF2MBopt2MBϕ.

The charge distribution in the complex (shown in Tab. IV) is sensitive to the presence of the phenyl rings. Calculation HF2MBopt2MB shows the metal to be the site of most positive charge (0.288) while in calculation HF2MBopt2MBϕ the site of most positive charge is C13 (0.0834). Again a more complete input for the calculation leads to the assignment of carbon 13 as the site of most positive charge.

Shown in Table V are the contributions to the LUMO of calculation HF2MBopt2MBϕ, which indicate that the orbital is mostly localized on the metal, with some contributions from the butadienyl ligand.

Nucleophiles

In determining whether a reaction is charge or orbital controlled, it is important to consider the energy difference between the HOMO of the nucleophile and the LUMO of the substrate. To this end, molecular orbital calculations were carried out on the hard (cyanoborate ion) and the soft (malonate ion) nucleophiles experimentally known to attack the complex. The geometry of both ions was optimized at the HF LANL2DZ level.

The majority of the electron density in the HOMO of the malonate ion is on the central carbon atom of the molecule; the orbital also includes a π antibonding interaction between the oxygen atoms and the central carbon. The HOMO of the cyanoborate ion is a delocalized π bonding interaction among all non-hydrogen atoms.

Determination of the Site of Attack

The substrate calculation chosen to determine the site of nucleophilic attack is calculation HF2DZopt2DZ, in which the highest basis set (LANL2DZ) was employed for both the geometry optimization and the HF calculation.

TABLE VI Energy differences between the LUMO of the substrate and the HOMO of the nucleophiles

HOMO (*a.u.*)	*LUMO* (*a.u.*)	ΔE (*a.u.*)	ΔE (*eV*)
Cyanoborate ion	calculation HF2DZopt2DZ		
−0.214	−0.063	0.151	4.11
Malonate ion	calculation HF2DZopt2DZ		
−0.131	−0.063	0.068	1.85

Shown in Table VI is the energy difference between the HOMO of each nucleophile and the LUMO of the complex. There is a smaller energy difference (1.85 eV) between the malonate ion and the complex than between the cyanoborate ion and the complex (4.11 eV). However, in both cases the difference is small, indicating that both nucleophilic attacks are orbital controlled. This implies that both nucleophiles attack the substrate at the site where the LUMO of the complex is localized.

Since the LUMO of calculation HF2DZopt2DZ receives its highest contribution from the metal, with a smaller contribution from C13 on the butadienyl ligand, both nucleophiles should attack at the metal. In fact, the hard nucleophile does; however, the soft nucleophile is more sterically demanding. It is therefore easier for the malonate ion to choose the site which has the second-largest contribution to the LUMO of the substrate and is sterically less hindered: C13 on the butadienyl ligand.[1] Experimental results confirm this conclusion.

CONCLUSIONS

A series of molecular orbital calculations were performed on the substrate molecule $[(\eta^3\text{—}CH_2C(CH_3)C{=}CH_2)Pt(PPh_3)_2]^+$. The theoretical approaches used were Hartree–Fock and X-α, employing LANL2MB and LANL2DZ basis sets. The choice of basis set seemed to have the biggest effect on the charge distribution of the molecule (see Tab. IV). On the other hand, the effect of basis set size and inclusion or exclusion of phenyl substituents in the phosphine ligands on the geometry optimization was minimal. Green *et al.*, suggested three resonance structures which could describe the bonding in the complex [7] (see Fig. 5). The best calculation in this work (calculation HF2DZopt2DZ) suggests that resonance

---

[1] Alternatively, the malonate ion could attack at the metal center, with the complex then rearranging to the observed product [2].

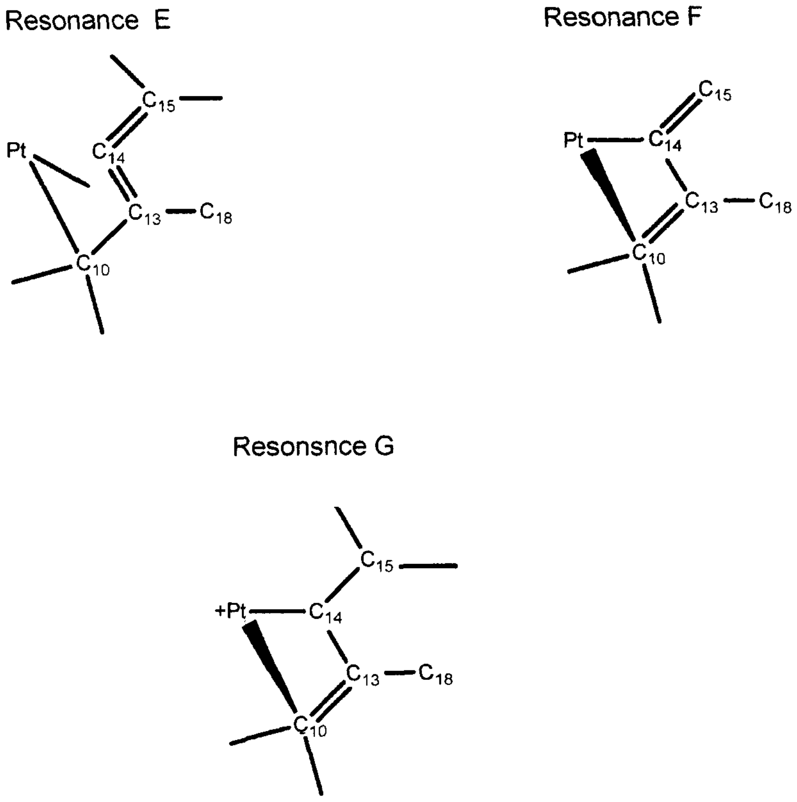

FIGURE 5 Resonance hybrids suggested by Greene *et al.* [7].

structure F makes the most important contribution to the bonding of the complex (see Fig. 3).

Calculations on two different nucleophiles (one hard and one soft) were used to determine the most likely site of attack on the substrate. Both reactions appear to be orbital controlled, which points to the metal as the preferred site of attack. However, the soft nucleophile attacks at the middle carbon of the allyl ligand because of steric factors.

Acknowledgements

We are grateful to the Pittsburgh Supercomputing Center for allowing us access to their Digital Alpha 3000 and DEC station 5000 systems through grant # CHE950011P.

References

[1] M. Green, S. A. Benyunes, L. Brandt and A. W. Parkins, *Organometallics* **10**, 57 (1991).

[2] R. H. Crabtree, *The Organometallic Chemistry of the Transition Metals* (John Wiley & Sons, 2nd edition, 1994).

[3] B. E. Douglas, *Concepts and Models of Inorganic Chemistry* (John Wiley & Sons, 2nd edn., 1983).

[4] G. J. Klopman, *J. Am. Chem. Soc.* **90**, 223 (1968).

[5] Gaussian 94, Revision C.2, M. J. Frisch, G. W. Trucks, H. B. Schlegel, P. M. W. Gill, B. G. Johnson, M. A. Robb, J. R. Cheeseman, T. Keith, G. A. Peterson, J. A. Montgomery, K. Raghavachari, M. A. Al-Laham, V. G. Zakrewski, J. B. Foresman, J. Cioslowski, B. B. Stefanov, A. Nanayakkra, M. Challacombe, C. Y. Peng, P. Y. Ayala, W. Chen, M. W. Wong, J. L. Andres, E. S. Replogle, R. Gonperts, R. L. Martin, D. J. Fox, J. S. Binkley, D. Defrees, J. Baker, P. Stewart, M. Head-Gordon, C. Gonzalez and J. A. Pople, Gaussian, Inc., Pittsburgh PA, 1995.

[6] (a) H. B. Schlegel, *J. Comp. Chem.* **3**, 214 (1982); (b) H. B. Schlegel, *New Theoretical Concepts for Understanding Organic Reactions*, Ed. J. Bertran (Kluwer Academic: The Netherlands, 1989); (c) H. B. Schlegel, "Geometry Optimization on Potential Energy Surfaces", In: *Modern Electronic Structure and Theory*, Ed. D. R. Yarkony (World Scientific Publishing: Singapore, 1994).

[7] S. A. Benyunes, L. Brandt, A. Fries, M. Green, M. F. Mahon and T. M. T. Papworth, *J. Chem. Soc. Dalton Trans.* p. 3785 (1993).

[8] P. J. Hay and W. R. Wadt, *J. Chem. Phys.* **82**, 270 (1985).

[9] W. J. Hehre, R. F. Stewart and J. A. Pople, *J. Chem. Phys.* **51**, 2657 (1969).

[10] J. B. Collins, P. v. R. Schleyer, J. S. Binkley and J. A. Pople, *J. Chem. Phys.* **64**, 5142 (1976).

[11] W. J. Hehre, L. Radom, P. v. R. Scheleyer and J. A. Pople, *Ab Initio Molecular Orbital Theory* (John Wiley & Sons, 1985).

[12] J. C. Slater, *Adv. Quantum Chem.* **6**, 1 (1972).

[13] K. H. Johnson, *Adv. Quantum Chem.* **7**, 143 (1973).

[14] (a) P. Hohenberg and W. Kohn, *Phys. Rev.* **136**, B864 (1964); (b) W. Kohn and L. J. Sham, *Phys. Rev.* **140**, A1133 (1965); (c) J. C. Slater, *Quantum Theory of Molecules and Solids* (Vol. 4, McGraw-Hill, 1974).

[15] (a) M. C. Milletti and D. Curtis, *Polyhedron* **9**, 1855 (1990); (b) M. C. Milletti, *Polyhedron* **12**, 401 (1992); (c) M. C. Milletti, *Polyhedron* **16**, 3663 (1997).

[16] R. S. Mulliken, *J. Chem. Phys.* **23**, 1997 (1955).

[17] (a) M. Guerra, D. Jones, G. Distefano, A. Foffani and A. Modelli, *J. Am. Chem. Soc.* **110**, 375 (1988); (b) M. Guerra and D. Jones, *Organometallics* **12**, 2203 (1993); (c) M. C. Bohm, R. Gleiter and C. D. Batich, *Helv. Chim. Acta* **63**, 990 (1980).

[18] (a) E. J. Baerends, C. Oudahoorn and A. J. Oskam, *J. Electron Spectrosc. Rel. Phenom.* **6**, 259 (1975); (b) A. Modelli, G. Distefano, M. Guerra and D. Jones, *J. Am. Chem. Soc.* **109**, 4440 (1987); (c) M. F. Ouest, I. H. Hillier, B. R. Higginson and D. R. Llyod, *Mol. Phys.* **29**, 113 (1986); (d) J. H. Osborne, W. C. Trogler, P. D. Moran and C. G. Francis, *Organometallics* **6**, 94 (1987).